



Article

# Traffic-Based Heuristics for Regenerator Placement in Translucent Dynamic Optical Networks

Andre L. S. de Farias <sup>1</sup>, Raul C. Almeida, Jr. <sup>2</sup> and Daniel A. R. Chaves <sup>1,\*</sup>

<sup>1</sup> Computer Engineering Department, Polytechnic School of Pernambuco, University of Pernambuco, Recife 50740-540, PE, Brazil; farias.andre@outlook.com

<sup>2</sup> Department of Electronics and Systems, Federal University of Pernambuco, Recife 50740-540, PE, Brazil; raul.almeidajunior@ufpe.br

\* Correspondence: darc@comp.poli.br

**Abstract:** We propose in this paper two heuristic strategies to solve the regenerator placement problem (RPP) in translucent networks under dynamic traffic. The heuristics are based on both the forecast of the offered load and estimates of blocking probabilities in the network nodes. The proposed heuristics are compared to other regenerator placement algorithms from the literature in two different topologies. The results show that one of the proposed algorithms outperforms, in the investigated scenarios, all other algorithms from the literature considered for comparison purposes in this paper, whereas the second proposed algorithm outperforms the algorithms from the literature only in some considered scenarios.

**Keywords:** translucent optical networks; regenerator placement; dynamic traffic; heuristics; network design; sparse regeneration; 3R; regenerator



**Citation:** de Farias, A.L.S.; Almeida, R.C., Jr.; Chaves, D.A.R. Traffic-Based Heuristics for Regenerator Placement in Translucent Dynamic Optical Networks. *Appl. Sci.* **2022**, *12*, 4388. <https://doi.org/10.3390/app12094388>

Academic Editor: Giuseppe Rizzelli

Received: 27 February 2022

Accepted: 21 April 2022

Published: 27 April 2022

**Publisher's Note:** MDPI stays neutral with regard to jurisdictional claims in published maps and institutional affiliations.



**Copyright:** © 2022 by the authors. Licensee MDPI, Basel, Switzerland. This article is an open access article distributed under the terms and conditions of the Creative Commons Attribution (CC BY) license (<https://creativecommons.org/licenses/by/4.0/>).

## 1. Introduction

The technology of dense wavelength division multiplexing (DWDM) divides the available fiber spectrum into wavelength bands named as channels [1,2]. The optical networks that use DWDM technology and perform optical-electrical-optical (O/E/O) conversion in all intermediate nodes of each lightpath are known as opaque networks [1]. These networks usually show a good performance in terms of blocking probability (BP) but require high capital expenditure (CapEx) for their installation due to the large amount of transponders deployed in their nodes [3,4]. In transparent all-optical networks, on the other hand, the O/E/O is not performed in the lightpaths' intermediate nodes, which results in a lower implementation CapEx. However, the signal may be excessively degraded due to physical-layer penalties. These penalties may be mitigated by the use of 3R regenerators [1]. Such regenerators are used whenever the accumulated penalties make the signal quality of transmission (QoT) unacceptable [1,4]. The QoT is usually verified by using either the optical signal to noise ratio (OSNR) [4] or the maximum optical reach (MOR) [2]. MOR is the maximum distance that the optical signal can propagate, keeping the bit error rate (BER) under a certain limit.

The use of 3R alongside a lightpath divides it into transparent segments (TS). The signal propagates with no O/E/O conversions along each TS. The networks that use 3Rs in some of their routes are known as translucent optical networks [1]. These networks aim to find a good CapEx/performance trade-off, drawing the main advantages of both opaque and transparent networks. The algorithm responsible for dividing the lightpath into TS segments is known in the literature as the regenerator assignment (RA) procedure [5–7].

The design of translucent optical networks is a multi-objective problem that needs to deal with two conflicting aspects: the capital cost and the performance improvement. The performance improvement generated by the inclusion of 3R regenerators in the network can be evaluated by reducing the network blocking probability. The cost aspect can be

evaluated by the number of regeneration devices installed in the network. The capital cost related to including a large number of regenerators can be of the same order of magnitude as the capital cost required to install all other equipment needed to build the entire optical network [8]. For this reason, the network carriers tend to use as few regenerators as they can in their networks to reduce their costs.

To perform the design of translucent networks, it is important to consider the type of traffic embedded in the network. One can broadly classify the types of traffic as deterministic (also known as static) and stochastic (also known as ad-hoc or dynamic) [9]:

- deterministic/static traffic—the parameters of all network demands are known in advance and they are deterministic information. These parameters for each demand are the source and destination nodes, setup time (start time of the connection), and the disconnection time (end time of the connection). The list of all demands with their information is the traffic matrix.
- ad-hoc/dynamic traffic—the parameters of all network demands, such as source and destination nodes, setup time, and disconnection time, are all unknown, i.e., they are random variables. The clients' connections are requested to the network, on-demand, in an intempestive manner. In this case, usually, the traffic matrix consists of the list of values for each source and destination node used to state stochastic modeling for the traffic.

The design of a translucent network often uses one of two approaches: islands of transparency or sparse distribution [1]. In using the sparse distribution, the network design determines how the regenerators should be distributed among the network nodes. This problem is known in the literature as the regenerator placement problem (RPP). There are three main approaches to solving the RPP [9–11]:

- RPP-1—given a physical topology and a deterministic traffic matrix (static traffic), find the minimum number of regenerators that should be placed in the network nodes to embed in the network all demands present in the traffic matrix, such that all demands can be routed in the network using a path formed by TSs smaller than MOR.
- RPP-2—Given a physical topology and source-destination pairs of all demands listed in the traffic matrix, find the minimum set of network nodes that must have regenerators such that all demands may be routed in the network using a path formed by TSs smaller than MOR.
- RPP-3—Given a physical topology, an ad-hoc traffic matrix and a total number of regenerators that should be deployed in the network, find the number of regenerators that should be placed in each network node to minimize the network blocking probability. In RPP-3, the regenerators are deployed in each network node and they are assigned (used) to each path, on-demand, according to the necessity of the incoming lightpath to be divided into TSs smaller than MOR. Thus, in a given time, there are both assigned (used) and unassigned (free) regenerators in each network node. Eventually, a demand that requires a route longer than the MOR (i.e., it requires regeneration) may be routed throughout nodes with no free regenerators, which causes blocking of the demand.

The three mentioned RPP versions are computationally complex and classified either as NP-complete or NP-hard [4,9–11]. Thus, heuristics [3,12] or meta-heuristics [4,11,13] are often used to solve RPP. Note, however, that the minimization target of RPP-1 and RPP-2 has a linear characteristic (either sum of the number of regenerators deployed or sum of nodes with regeneration capability) and, for this reason, there are several approaches in the literature using (M)ILP to solve either RPP-1 [10,14] or RPP-2 optimally [9,15–20]. Typically, however, (M)ILP methods solve the problem for networks with a low number of nodes [9,10,15–17]. In RPP-3, on the other hand, the minimization target is the network blocking probability. Clearly, the network blocking probability has a non-linear dependence on the number of regenerators deployed in each network node which prevents the use of (M)ILP methods to solve the RPP-3 problem optimally. To optimally solve the RPP-3,

BP modeling is required. Very few BP modelings for translucent networks are available in the literature and they assume several simplifications to reach a very complex (and computationally intensive) set of formulas [21]. This fact prevents using an optimization method over this set of equations to solve RPP-3 in an acceptable time optimally.

In this paper, we are interested in addressing networks under ad-hoc traffic. Clearly, RPP-1 can only solve the design of networks under static traffic. RPP-2, on the other hand, can be used to resolve networks with ad-hoc traffic. However, it cannot do the optimization to reduce BP, nor with the objective of reducing the network implementation cost because it only defines which nodes in the network must have regenerators without answering how many regenerators should actually be installed on each node. Thus, the only approach capable of handling the optimization of both performance (BP) and capex (cost) for networks under ad-hoc traffic is the RPP-3. In this paper, we focus on solving RPP-3, hereafter named as RPP, under ad-hoc traffic. For this reason, we used, in this paper, the heuristic approach to solve the RPP.

The Poison/Markovian process using exponential distribution for connection request inter-arrival and holding times are largely assumed in the literature to model the ad-hoc/dynamic traffic in optical circuit-switched networks [1,2,11–13,16,21–24]. Nevertheless, some classical works [25] bring to attention the self-similar characteristics of data networks traffic, pointing out the inadequacy of the Poison/Markovian process to characterize such network traffic. However, based on observation of actual data traffic, more recent papers have shown that the Poison/Markovian process can closely represent the traffic of current high-speed backbone networks data traffic, mainly because the burstiness of the inter-arrival times decreases significantly in current backbone networks [26–28].

There are two main approaches to solving RPP-3 under ad-hoc traffic heuristically: (1) using either topological or traffic characteristics of the network (such as the degrees of the nodes, number of routes that pass through a node, etc.) to infer the amount of regenerators that should be placed in each node to reduce the BP or (2) using the BP returned by a network simulator and applying this information as a guide during the regenerator placement. The disadvantage of the strategies that use the first approach [1,2,4,12,22,29] is that they do not consider BP information during the RPP solution.

Strategies that use the second approach [11,13,30], on the other hand, take into account BP information during the RPP decision. However, they require a network simulator to return those BPs, which may lead to large complexity and excessive time to reach the RPP solution. In this paper, we propose solving the RPP using the second approach but dismissing the use of network simulations to return the related BPs during the RPP procedure. Instead, for the BP evaluation, we use approximate analytical modeling, which allows the evaluation of the impact of the inclusion of each regenerator in the overall network BP.

Using the heuristic approach, Pedro [2] proposes a statistical framework to tackle RPP in translucent optical networks under ad-hoc traffic. The framework consists of two parts: first, some heuristic is used to evaluate the probability  $pdf_{3R}(i)$  of a node  $i$  being used as a regeneration point by some lightpath. Then, the regenerators are iteratively placed in the network, one per iteration, in the node that presents the maximum value of the following deviation:  $\Delta pdf_{3R}(i) = pdf_{3R}(i) - n_{3R}(i)/n_{3R}^{total}$ , in which,  $n_{3R}(i)$  is the current number of regenerators deployed in node  $i$  and  $n_{3R}^{total}$  is the total number of regenerators to be deployed in the network.

In this paper, we propose two heuristics to solve RPP. We introduce two alternative approaches based on Markov modeling to evaluate  $pdf_{3R}(i)$ , and we propose that during the iterative process, the decision to place a regenerator on a node be based on the BP reduction generated by that choice. To infer the BP reduction, we used a predicted ad-hoc traffic matrix used to model the stochastic behavior of the ad-hoc traffic. Different from the algorithms presented in [2], the proposed strategies can also consider non-uniform traffic. We also introduce the concept of the essential node, which helps solve RPP. Thus, the main contribution of our method is that we approximately evaluate the reduction of

the overall network blocking probability (BP) caused by the addition of a regenerator in each network node and we select, for the 3R inclusion, the node that provides the greatest reduction in BP. The previous methods, on the other hand, do not perform such evaluation: they usually place regenerators proportionally to the traffic offered to each node, which does not correspond to the solution that results in the greatest reduction of the BP because the relationship between the reduction in BP and node offered load is not linear.

The paper is organized as follows: in Section 3, we establish some definitions and mathematical notation used in the paper, in Section 4, we introduce the proposed RPP heuristics, in Section 5, we state the simulation setup used in the simulations, in Section 6 we show the simulation results and in Section 7, we give our conclusions.

## 2. Related Works

In this work, we propose two new approaches to perform sparse regenerator placement in translucent optical networks under ad-hoc/dynamic traffic. Thus, we deal with the problem defined in Section 1 as RPP-3. Note, however, that there are few works in the literature that fully realize the RPP-3 goals by using the network blocking probability information to guide the regenerator placement itself. In this section, we review some algorithms proposed in the literature seeking the solution to RPP-3. Two main types of algorithms are reviewed, the algorithms that fully accomplish the RPP-3 goals (RPP-3d) as well as those that do not use the blocking probability information directly during the placement decision but, instead, apply heuristics whose ultimate goal is to reduce the network blocking probability (RPP-3h).

Yang and Ramamurthy [1] propose four different heuristic algorithms to solve the RPP. Each heuristic assigns a score to each network node and the  $N$  best-scored nodes receive a predetermined number of  $X$  regenerators ( $N-X$  policy). The proposed NDF and CNF algorithms give the score for each network node based, respectively, on the node degree and on how centered in the network the node is. These are topological-based heuristics because only information from the network topology is used during the placement decision. The work also proposed the TLP and SQP traffic-based heuristics. They are traffic-based heuristics because a set of dynamic call requests are simulated to evaluate each network node score. The TLP scores the network node  $i$  based on the number of times that a call request is routed through the node  $i$  and the SQP does the same but considering the transparent reach in terms of the number of hops.

Some other traffic-based placement proposals use a similar idea and a network simulation engine to simulate a set of dynamic call requests. The statistics of node usage during the simulations are used to score the network nodes towards a regenerator placement decision. Applying this idea, Chaves et al. [4] proposed the MU and MSU heuristics and Walkowiak et al. [29] proposed the SAUR heuristic. The MU scores each node  $i$  based on the number of times that the node  $i$  is assigned as a regeneration point during the simulation, whereas the MSU algorithm scores each node  $i$  based on the maximum number of regenerators simultaneously assigned in the node  $i$  during the simulation. In both cases, the total number of regenerators to be deployed in the network are distributed among the network nodes proportionally to each node score. The SAUR heuristic further improves the MSU idea by taking into account not only the number of simultaneously used regenerators in a node but also the statistics regarding the usage.

As mentioned in Section 1, Pedro [2] proposes a statistical framework to tackle RPP-3h in translucent optical networks under ad-hoc traffic. The mentioned  $pdf_{3R}(i)$  function is evaluated accordingly to the selected heuristics. He proposes to evaluate the  $pdf_{3R}(i)$  considering only topological information such as node degrees and shortest paths between each pair of nodes. Thus, only the topological-based placement is considered in the work. The  $pdf_{3R}(i)$  is evaluated using four different strategies: (1) equal value for all nodes (UN); (2) proportionally to the node degree (ND); (3) proportionally to the number of shortest paths that pass through the node  $i$  (RO); (4) the same as RO but also considering the transmission reach (RR).

Moreover, applying topological-based placement, Aibin and Walkowiak [12] propose the DA heuristic. This heuristic also assigns a score to each network node. The score of the node  $i$  is evaluated by the quotient between the sum of the lengths of the links connected to the node  $i$  by the total length of all links in the network. Then, the regenerators are distributed proportionally to each node score.

The algorithms reviewed so far apply the RPP-3h approach. On the other hand, Cavalcante et al. [11] and Chaves et al. [13] apply a genetic-algorithm-based solution to solve a multi-objective version of the RPP-3d problem for, respectively, elastic and WDM optical networks. Based on the forecast traffic matrix, the algorithm seeks to find the regenerator placement solution which achieves the best trade-off between the total number of deployed regenerators and the network blocking probability. These algorithms reach lower blocking probabilities than other placement algorithms in the literature. The traffic information and the total network blocking probability are used to influence the placement decision itself, but a network simulator engine is needed to assess each solution proposed by the genetic algorithm during the regenerator placement procedure.

Zhao et al. [21] propose analytical models for computing the blocking performance of translucent optical networks with sparsely located regeneration nodes. The analytical models developed to estimate the call blocking probability in an optical network are applied to assess two regeneration node allocation policies. The proposed analytical models are suitable to be used to assess the translucent optical network performance, but they are computationally complex enough to prevent its use during the translucent network design (regenerator placement decision) because several different placement combinations must be investigated during the designing procedure.

The results from the above-reviewed papers consistently show that traffic-based placement approaches achieve lower blocking probabilities in comparison to topology-based approaches. Traffic-based approaches can also satisfactorily solve the placement problem for the network under both uniform and non-uniform traffic patterns, whereas the topology-based approaches give the same result regardless of the offered traffic pattern. All reviewed traffic-based approaches require a network simulator engine to simulate a realistic per node regenerator demand (in the case of the application of RPP-3h) [1,4,29] and its resultant network blocking probability (in the case of the application of RPP-3d) [11,13]. Different from the other algorithms in the literature, we propose in this paper an approximate analytical model to evaluate the network blocking probability and we employ this model during the placement procedure. Our heuristic proposals use the blocking probability information to guide the regenerator placement. The proposed heuristics are traffic-based placement algorithms that can, at the same time, heuristically solve RPP-3d, deals with uniform and non-uniform traffic patterns, and dismiss the use of a simulator engine during the regenerator placement decision.

### 3. Definitions

This section specifies the notations used to describe the proposed RP heuristics presented in Section 4.

#### 3.1. Premises and Notation

Suppose a network with  $N$  nodes and MOR given by  $T_R$ . The route between nodes  $i$  and  $j$  is defined as  $\pi_{ij} = [n_1, n_2, \dots, n_{H_{ij}}]$ , where  $H_{ij}$  is the number of nodes in the route. Let us assume that  $\pi_{ij}$  has a total physical length  $T_{ij}$  and a total optical length  $V_{ij} = T_{ij} + (H_{ij} - 2) \cdot \epsilon$ . The optical length accounts for the physical length added by an extra  $\epsilon$  length per intermediate node, representing the degradation suffered by the signal passing through these nodes [2]. Using  $\pi_{ij}$ ,  $V_{ij}$  and  $T_R$ , it is possible to determine the minimum number of regenerators,  $K$ , that keeps the optical length of all  $K + 1$  resultant TSs in  $\pi_{ij}$  shorter than  $T_R$ .

For a network under ad-hoc traffic, lightpaths are set up and torn down dynamically. In these networks, the traffic is usually assumed memoryless and evaluated in an erlang



unit, defined as the ratio between the average connection holding time and the average time between requests. The ad-hoc traffic matrix is represented in this paper as  $\Omega = \{\omega_{ij}\}$ , such that  $\omega_{ij}$  represents the traffic between nodes  $i$  and  $j$  (in erlang unit), with  $\omega_{ij} = 0$  if  $i = j$  and the total network load is  $L = \sum_{i=1}^N \sum_{j=1}^N \omega_{ij}$ . The traffic matrix that considers only those paths  $\pi_{ij}$  that require mandatory regeneration (i.e.  $V_{ij} > T_R$ ) is  $\Gamma = \{\gamma_{ij}\}$ , in which  $\gamma_{ij} = \omega_{ij}$  if  $V_{ij} > T_R$  and  $\gamma_{ij} = 0$  otherwise.

### 3.2. Set of Possible Regenerator Combinations (PRC)

A regenerator combination of a route is a combination of nodes in the route that satisfies the criteria that all TSs formed with the signal regeneration in such nodes are feasible, i.e., their optical lengths are shorter than  $T_R$ . Let  $C_{ij}$  be the set of all those regenerator combinations on route  $\pi_{ij}$  that use the minimum number of possible regeneration points,  $K_{ij}$ , i.e.,:

$$C_{ij} = [(n_1^{(1)}, \dots, n_{K_{ij}}^{(1)}) \dots (n_1^{(M_{ij})}, \dots, n_{K_{ij}}^{(M_{ij})})] \\ = \{c_{ij}^{(1)}, \dots, c_{ij}^{(M_{ij})}\}, \tag{1}$$

in which  $M_{ij}$  is the number of regenerator combinations of  $\pi_{ij}$  and  $n_k^{(m)}$  is the  $k$ -th selected regeneration node along the route  $\pi_{ij}$  of the  $m$ -th regenerator combination.  $C_{ij}$  is defined as the possible regenerator combinations (PRC). It stores all regenerator combinations that segment the route  $\pi_{ij}$  into  $K_{ij} + 1$  feasible transparent segments. Notice that  $M_{ij} \leq \binom{H_{ij}-2}{K_{ij}}$ , since  $H_{ij} - 2$  is the number of intermediate nodes where regeneration can take place and  $K_{ij}$  is the number of nodes using regeneration.

### 3.3. Set of Feasible Regenerator Combinations (FRC)

In a typical translucent network, some nodes in the network may not have installed regenerators. In addition, even in nodes with installed regenerators, they may all be busy (i.e., in use) on the arrival of a connection request. Thus, a possible regenerator combination (as defined in Section 3.2) is referred to as feasible only if all of its nodes have at least one regenerator installed and it is free on the arrival of a request. We may define a subset  $D_{ij} \subseteq C_{ij}$  that considers only the feasible regenerator combinations in  $C_{ij}$ .  $D_{ij}$  is formed by  $M'_{ij} \leq M_{ij}$  feasible regenerator combinations in  $C_{ij}$ , described as

$$D_{ij} = [(n_1^{(1)}, \dots, n_{K_{ij}}^{(1)}) \dots (n_1^{(M'_{ij})}, \dots, n_{K_{ij}}^{(M'_{ij})})] \\ = \{d_{ij}^{(1)}, \dots, d_{ij}^{(M'_{ij})}\}, \tag{2}$$

in which  $d_{ij}^{(m)}$  is one of the feasible regenerator combinations. If  $H'_{ij}$  is the number of intermediate nodes in  $\pi_{ij}$  with at least one installed and free regenerator (note that  $H'_{ij} \leq H_{ij} - 2$ ), we have that  $M'_{ij} \leq \binom{H'_{ij}}{K_{ij}}$ .

### 3.4. Essential Nodes

Using the PRC set, it is possible to define the concept of essential node. Node  $n_u$  is defined as essential for the route  $\pi_{ij}$  if  $n_u \in c_{ij}^{(m)}$  for all values of  $m$  ( $1 \leq m \leq M_{ij}$ ). In other words,  $n_u$  is essential if it participates in all PRCs of  $\pi_{ij}$ . Note that it is mandatory to place regenerators in essential nodes because, otherwise, some routes become unfeasible in terms of QoT. For this reason, the proposed algorithms in this work start by placing regenerators in the essential nodes.

#### 4. Proposed Regenerator Placement Heuristics

The regenerator placement heuristics proposed in this paper are based on: (1) defining either the possible or feasible regenerator sets for each source-destination node pair, as described in Sections 3.2 and 3.3, respectively; (2) estimating the load offered to each node by considering only the load of the routes which demand regeneration, and (3) Given the estimated load per node and the number of regenerators installed per node, estimate the overall network blocking probability mitigation when a new regenerator is installed in a specific node.

In this section, we propose two strategies to solve RPP. The proposed strategies coincide in steps (1) and (3) and differ in the form of how the offered load to each network node is estimated. We describe in Section 4.1 how the offered load to a node is estimated in the proposed strategies. It is important to mention that the load and blocking probabilities estimates presented in Sections 4.1 and 4.2 are not intended to give an exact evaluation of such values. Instead, they are intended to be used as an approximate, although precisely enough, estimate so that an efficient heuristic approach to solve RPP may be built.

Although both proposals consider the network traffic pattern forecast and intensity as input information to solve RPP; they can provide efficient regenerator placement even when the actual network traffic is moderately different from that one forecast, as discussed in the results section.

##### 4.1. Estimation of the Total Regeneration Load Offered to a Node

The load offered to the pool of regenerators installed in the network node  $n$  can be roughly estimated by the sum of the loads of all lightpaths that need regeneration and pass through that node. This sum can be evaluated as

$$\beta_n = \sum_{i=1}^N \sum_{j=1}^N G_{ij}(n), \tag{3}$$

in which  $G_{ij}(n) = \gamma_{ij}$  if  $\exists m / n \in c_{ij}^{(m)}$  and 0 otherwise.

It is possible to improve the  $\beta_n$  estimate by considering that the offered load  $\gamma_{ij}$  is proportionally distributed among all FRCs. The reasoning for this is that two FRCs cannot be used simultaneously. For instance, if there are three feasible combinations for  $\pi_{ij}$ , then the offered load for each combination is approximately  $\gamma_{ij}/3$ . The estimate of the total effective offered load to node  $n$  can be evaluated by

$$\alpha_n = \sum_{i=1}^N \sum_{j=1}^N F_{ij}(n), \tag{4}$$

in which

$$F_{ij}(n) = \begin{cases} \frac{\gamma_{ij}}{M'_{ij}} \sum_{m=1}^{M'_{ij}} P_{ijm}(n), & \text{if } n \in \pi_{ij} \\ 0, & \text{otherwise,} \end{cases} \tag{5}$$

with  $P_{ijm}(n) = 1$  if  $n \in d_{ij}^{(m)}$  and 0 otherwise. In this paper, it is proposed to evaluate the  $pdf_{3R}(n)$  (using the notation from [2]) by either:  $\beta_n / \sum_{i=1}^N \beta_i$  or  $\alpha_n / \sum_{i=1}^N \alpha_i$ .

##### 4.2. Blocking Probability Estimation

Consider a node  $n$  with  $r(n)$  regenerators installed and the estimate of its offered load given by  $\Gamma_n$  ( $\Gamma_n$  as a place holder for either  $\alpha_n$  or  $\beta_n$ ). Node  $n$  can be seen as a pool of  $r(n)$  servers under an offered load  $\Gamma_n$ . In such a case, the probability that node  $n$  has no available regenerator on the arrival of a request can be evaluated as:  $BP(n) = B(r(n), \Gamma_n)$ , in which  $B(s, a)$  is the Erlang B formula, derived using the Markov chain theory [31], that returns the blocking probability (BP) of a system with  $s$  servers under an offered load  $a$ .

To choose which node the regenerator shall be installed on, it is important to quantify the impact that the addition of a regenerator in each network node causes on the network path request blocking probability. As known in Markov theory, the blocking probability of a node  $n$ ,  $BP(n)$ , is the long-term proportion of time that the node spends without an available regenerator. Therefore, the number of requests that require a regenerator at node  $n$  and are blocked is proportional to  $BP(n)$  multiplied by the total requested traffic. We may then think about quantifying the portion of the overall network BP that is caused by blocking imposed on the paths that use node  $n$  as a regeneration point.

Let us assume that each path  $\pi_{ij}$  that may use a regenerator in node  $n$  experiences approximately a blocking probability given by  $BP(n)$ . Using  $E_{ij}(n)$  as a place holder for either  $G_{ij}(n)$  or  $F_{ij}(n)$ , it is possible to estimate the amount of the overall network BP only due to the blocking caused by node  $n$  as

$$BP_N(n) = \frac{\sum_{i=1}^N \sum_{j=1}^N B(r(n), \Gamma_n) \cdot E_{ij}(n)}{\sum_{i=1}^N \sum_{j=1}^N \omega_{ij}} \tag{6}$$

or

$$BP_N(n) = (\Gamma_n/L) \cdot B(r(n), \Gamma_n). \tag{7}$$

Thus, one may evaluate the network BP reduction caused by the inclusion of a single regenerator in the node  $n$  using

$$\Delta BP_N(n) = \frac{\Gamma_n}{L} ([B(r(n), \Gamma_n) - B(r(n) + 1, \Gamma_n)]). \tag{8}$$

The deviation shown in Equation (8) is used to decide which node receives a new regenerator at each algorithm iteration.

We provide in Appendix A a proposal to evaluate (8) considering a flexgrid/multiple rates demands scenario that occurs in elastic optical networks (EONs).

#### 4.3. Regenerator Placement Algorithms

The regenerator placement proposed in this paper is shown in Algorithm 1. The algorithm requires as input parameters the total amount of regenerators  $R$  to be deployed in the network, the forecast traffic matrices  $\{\omega_{ij}\}$  and  $\{\gamma_{ij}\}$  and the network topology. In the algorithm,  $\Gamma_n$  stands for either  $\alpha_n$  or  $\beta_n$  and  $\Delta(n) = \Delta BP_N(n)$ . First, the algorithm identifies and places one regenerator in each essential node. After that, it places one regenerator per iteration. The estimates of node offered load are re-evaluated in each iteration. The node that returns the highest BP reduction (i.e., the highest value for  $\Delta(n)$ ) receives one regenerator. Ties are broken, firstly by placing the regenerator in the node with the largest  $\Gamma_n$  and then randomly. The process is repeated until all regenerators are placed. Regarding the selection of  $\Gamma_n$ , two heuristics are proposed: Fixed Load Distribution (FLD), which uses  $\Gamma_n = \beta_n$  and Dynamic Load Distribution (DLD), which uses  $\Gamma_n = \alpha_n$ . Note that, in the particular case in which  $\Delta(n) = \Delta p d f_{3R}(n)$  and under uniform traffic, the FLD is equal to the Routing-&-Reach algorithm [2].

Our algorithm can be classified as traffic-based because the traffic matrices  $w_{ij}$  and  $\gamma_{ij}$  directly affect the decision of placing a regenerator in a given node. Please note in Algorithm 1 that the decision of placing a regenerator in a node depends on  $\Delta(n)$ , which, in the proposed algorithms, is evaluated as  $\Delta BP_N(n)$  by using Equations (6)–(8). Note that, in such equations, the estimated offered load  $\Gamma_n$  to a node and the current number of installed regenerators  $r(n)$  in a node are taken into account. Finally,  $w_{ij}$  directly appears in Equations (6) and (7), and the evaluation of the estimated offered load to a node,  $\Gamma_n$ , takes into account  $\gamma_{ij}$  by using either Equations (3) or (4).

#### 4.4. Time Complexity Analysis of the Proposed Algorithms

Let us start the analysis of the time complexity of the proposed algorithms by discussing the time complexity required to evaluate both the  $M_{ij}$  and  $M'_{ij}$  combinations. As



shown in Sections 3.2 and 3.3 for a route  $\pi_{ij}$ ,  $M_{ij} = \binom{H_{ij}-2}{K_{ij}}$  and  $M'_{ij} = \binom{H'_{ij}}{K_{ij}}$ . Note that, for each route, the value of  $K_{ij}$  is constant and known in advance. In such case, the evaluation of all combinations can be done in polynomial time if  $K_{ij}$  is not close to  $(H_{ij} - 2)/2$ , considering  $M_{ij}$  evaluation, and  $(H'_{ij}/2)$ , considering  $M'_{ij}$  evaluation. In a typical mesh optical network, it is expected that the signal may propagate for  $k$  hops before a regeneration is required (i.e., usually  $k$  is larger than 2). Therefore,  $K_{ij}$  is usually smaller than  $H_{ij}/2$ , which means that both  $M_{ij}$  and  $M'_{ij}$  can be evaluated in polynomial time. Even in the case in which  $K_{ij}$  is close to either  $(H_{ij} - 2)/2$  or  $H'_{ij}/2$ , the required time to evaluate both the  $M_{ij}$  and  $M'_{ij}$  combinations is low if  $H_{ij}$  is small. All routes with few (i.e., 2 to 5) hops fit in this case regardless of the number of hops the signal may traverse without regeneration. Typically, such cases represent the majority of the routes in a mesh optical network. Moreover, it is expected that the number of hops in a route can be considerably smaller than the number of nodes in the network. This is expected even for long routes. Thus, it could be concluded that the evaluation of the combinations is not prohibitive even for networks with a high number of nodes.

The most time-consuming step in Algorithm 1 is the  $\Gamma_n$  evaluation. It requires, in the worst case, finding the shortest path (SP) between all node pairs ( $\mathcal{O}(N^3)$ ) and, for each SP, the evaluation of either all PRCs (for FLD) or all FRCs (for DLD). By defining  $Z = \max_{i,j} M_{ij}$  (maximum number of PRCs) and  $Z' = \max_{i,j} M'_{ij}$  (maximum number of FRCs) we may write that the DLD shows  $\mathcal{O}(R \cdot N^3 \cdot Z')$  complexity whereas FLD (and Routing-&-Reach) shows  $\mathcal{O}(N^3 \cdot Z)$ . Note that DLD requires  $\Gamma_n$  reevaluation after each 3R inclusion and FLD does not. Given the above time complexities and the fact that  $M'_{ij} \leq M_{ij}$ , we can say, for the sake of comparison, that DLD requires, in the worst case,  $R$  times more time to solve the RPP problem than FLD.

---

**Algorithm 1** Pseudocode for proposed heuristics

---

**Require:** Total amount of regenerators to be deployed  $R$   
**Require:** Traffic matrices forecast  $\{\omega_{ij}\}$  and  $\{\gamma_{ij}\}$  and the topology

```

 $r \leftarrow R$ 
Determine all essential nodes
 $e \leftarrow$  Amount of essential nodes
 $r \leftarrow r - e$ 
Place one regenerator in each essential node
while  $r > 0$  do
  for  $n = 1$  to  $N$  do
    Place a temporary regenerator in node  $n$ 
    Evaluate  $\Gamma_n$  of all nodes
    Evaluate  $\Delta(n)$ 
    Remove the temporary regenerator placed at node  $n$ 
  Place one reg. in node  $n$  with highest value  $\Delta(n)$ 
   $r \leftarrow r - 1$ 

```

---

### 5. Simulation Setup

We use two topologies to evaluate the performance of the RPP algorithms: CoreNet (75 nodes and 99 bi-directional links) [32] and EuroNet (28 nodes and 41 bidirectional links) [33], both with 96 wavelengths per link, each transmitting 100 Gb/s PDM-QPSK. In the simulations, the transmission rate only affects the MOR and, unless stated otherwise, it is used the same values for 100 Gb/s adopted by Pedro [2]:  $T_R = 2000$  km, and  $\epsilon = 60$  km. However, we have also investigated the cases for  $T_R = 1600$  km,  $\epsilon = 60$  km and  $T_R = 2400$  km,  $\epsilon = 60$  km to validate the effectiveness of the proposed method under different transmission reaches.

Uniform traffic (UT) and non-uniform traffic (nUT) are considered during simulations. Under uniform traffic,  $\omega_{ij} = L/(N \cdot (N - 1))$  and under non-uniform traffic,

$\omega_{ij} = (\sigma_{ij} \cdot a \cdot L) / (N \cdot (N - 1))$ . The  $\sigma_{ij}$  is a random number uniformly distributed on the interval  $[0.5; 2.5]$  and the constant  $a$  is such that:  $a = (N \cdot (N - 1)) / (\sum_{i=1}^N \sum_{j=1}^N \sigma_{ij})$ . The random  $\sigma_{ij} \in [0.5; 2.5]$  means that the load between the nodes  $i$  and  $j$  for nUT traffic may vary from 50% to 250% of the load for the same pair under UT traffic, maintaining; however, the same total network load for both traffics.

There are two approaches mentioned in the literature and used in the industry to perform 3R in optical networks: (1) a shared pool of regenerators per node [1,2,11]; (2) the use of not assigned (i.e., free) add-drop interfaces to perform back-to-back regeneration [23]. In this paper, we assume that there is a pool of shared devices in each node exclusively dedicated to providing 3R capability and they can perform both wavelength conversion and signal regeneration.

The node architecture assumed in this paper is shown in Figure 1. It is composed by a colorless/directionless/contentionless (CDC) ROADM, de/multiplexers, add/drop interfaces, and a shared bank of 3R regenerators. Using this architecture, it is possible to decide, by using the ROADM switch fabric, whether the optical signal should be added/dropped, be bypassed, or undergo to the 3R shared bank to be regenerated. The node shown in Figure 1 supports a pair of fibers in each direction, the fibers arriving at the node are connected to ROADM switching fabric through the DEMUXes, whereas the fibers leaving the node are connected via MUXes. For example, signals from a client/user connected to a network node can be transmitted (or received) by accessing the “Add/Drop interfaces” block (bottom left in the figure). Then, they can be optically switched by ROADM to one of its outputs (or inputs), connected to a MUX (or DEMUX), until the signal may reach one of the output (or input) fibers of the node. On the other hand, an optical signal that is being transmitted along with the network and that arrives at a node (via fiber + DEMUX input) can be switched to an output port (via fiber + MUX output), or it can undergo electronic regeneration, being switched by the ROADM to the shared 3R regenerator bank (bottom right in the figure). In this case, the signal is regenerated by one of the 3R regenerators available in the bank and then inserted again into one of the input ports of the ROADM to be forwarded to one of the output fibers (fiber + MUX).

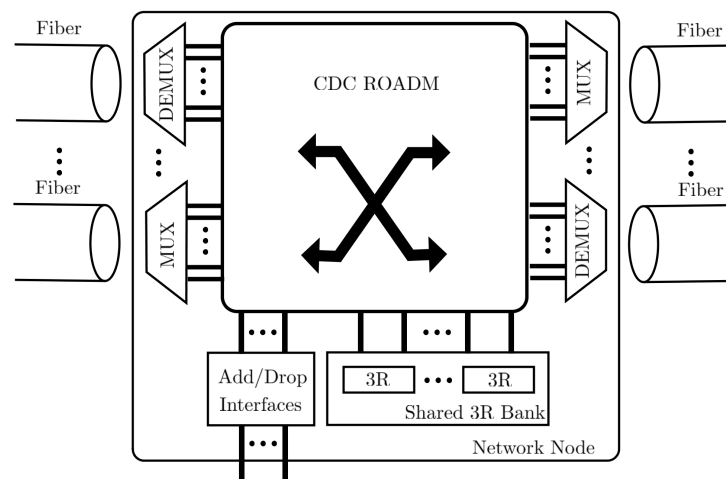


**Figure 1.** Node architecture assumed in this paper composed by a colorless/directionless/contentionless (CDC) ROADM, de/multiplexers, add/drop interfaces, and a shared bank of 3R regenerators (adapted from [2]).

The call requests are generated under a Poisson stochastic process in which the call duration follows an exponential distribution. Upon a call request, the shortest path (in terms of distance) from the source to the destination node is found using Dijkstra’s algorithm (we also investigated some cases using the k-shortest path routing algorithm as discussed in Section 6). The route is then segmented into TSs using the same RA used in [4] considering the MOR instead of OSNR as the QoT criterion. This RA uses regenerators to make feasible

routes with issues in either wavelength continuity constraints or QoT. The first fit algorithm performs wavelength assignment (WA) in each TS. If either RA or WA fails, the call is blocked; otherwise, the call is accepted.

In the blocking probability graphs shown in Section 6, the error bars for a confidence level of 95% are too small to appear in the graphs (smaller than the plot symbols used). It is obtained by repeating the same simulation point 30 times.

### 6. Results

We analyze in this section the performance of the proposed FLD and DLD algorithms to solve RPP and compare them with the following previously proposed strategies: Uniform (UN), Nodal-Degree (ND), Routing-Only (RO), and Routing-&-Reach (RR) [2]. In brief, all these algorithms distribute the  $R$  regenerators to each network node: uniformly (UN), proportional to the node degree of the node (ND), proportional to the number of shortest paths that pass through the node (RO), same as RO but also considering the transmission reach (RR). We also show the BP of the same network topologies, either transparent or opaque. Transparency occurs when no regenerators are installed in the network nodes. Opaqueness is achieved when all nodes are fully equipped with 3Rs. This requires a total of 19,008 regenerators installed in CoreNet and 7812 in EuroNet. In the simulated scenarios considering a transparent network (i.e., zero regenerator installed per node), we verified that the BP is dominated by the blockings due to paths  $\pi_{ij}$  with unacceptable values of  $T_{ij}$  (lack of reach), i.e., the blockings due to lack of wavelength are negligible in these scenarios. However, as the number of the deployed regenerators in the network increases, blockings occur due to both lack of reach and lack of wavelength. The relative values between these two blocking causes depend on the number of deployed regenerators.

Figure 2 (Figure 3) shows the BP as a function of the total number of regenerators installed in the CoreNet (EuroNet) topology under a load of 600 erl (500 erl), with Figure 2a (Figure 3a) standing for uniform traffic and Figure 2b (Figure 3b) standing for non-uniform traffic considered during the placement procedure. To evaluate how efficient are the proposed RPP procedures in cases where the traffic pattern used during the RPP process is different from the actual traffic offered to the network, we have investigated two situations: (1) The same traffic pattern is considered in the RPP procedure as well as in the BP evaluation (represented by symbols in the graphs) and (2) the traffic pattern for BP evaluation is different from the one considered during the RPP procedure (lines in the graphs). The case 1 has been named as the EQU scenario and case 2 as the DIF scenario. For each curve in the graphs, the traffic pattern considered during the RPP procedure is indicated after the  $p =$  symbol, whereas the traffic pattern considered during the BP evaluation is indicated after the  $s =$  symbol. For instance, DLD  $p = UT$   $s = nUT$  means that the DLD procedure placed the regenerators considering UT, whereas the BP was estimated for the network under nUT. This is an example of a DIF scenario. Note as well that the UN, ND, RO, and RR algorithms do not take into account any information regarding the traffic matrix, and we have used the notation  $p = *$  in such cases.

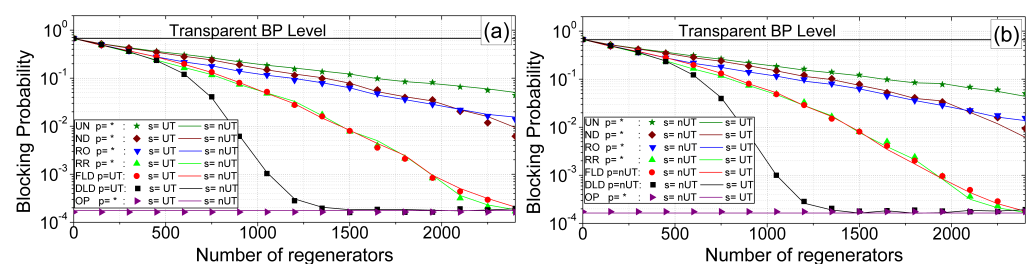


**Figure 2.** Blocking probability as a function of the total number of regenerators in CoreNet topology under 600 erlangs load and: (a) uniform and (b) non-uniform traffic.

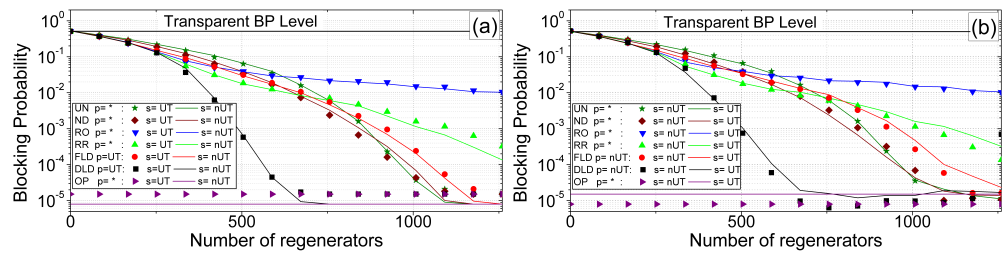


**Figure 3.** Blocking probability as a function of the total number of regenerators in EuroNet topology under 500 erlangs load: (a) uniform and (b) non-uniform traffic.

As expected, in Figures 2 and 3, the higher the number of deployed regenerators, the lower the BP found by the algorithms. Eventually, some algorithms reach a saturation point beyond which the placement of more regenerators results in no further reduction in BP. Note in Figures 2 and 3 that the DLD finds solutions that achieve significantly lower values of BP than all other investigated algorithms in both topologies and traffic patterns. Either FLD or RR algorithms find the second lowest values of BP in the entire investigated range in CoreNet and for low to a moderate number of regenerators in EuroNet. For a high number of deployed regenerators in EuroNet, on the other hand, the ND and UN algorithms present lower BP values than both FLD and RR.

Figure 2 (Figure 3) also shows that the DLD strategy can achieve with approximately 1330 (700) regenerators the same performance as an opaque CoreNet (EuroNet) network, whereas the second best algorithm, RR (ND), achieves the same level using 2090 (1100) regenerators. It means that the DLD can reach the opaque network BP level in the CoreNet (EuroNet) topology using only about 7% (9%) of the total regenerators required to mount an opaque network and using 63% (63% for UT and 74% for nUT) of the regenerators required by the second-best algorithm to reach the same level.

Figure 4 (Figure 5) shows, as an example, how the considered RPP algorithms distribute the regenerators along the network nodes in CoreNet (EuroNet) when a total of 1050 (504) regenerators are placed in the network considering UT. The figures show how many regenerators are placed in each node (according to its node ID). In both figures, one can observe that DLD, FLD, RR, and RO algorithms achieve a similar distribution of regenerators along the nodes. However, FLD, RR, and RO tend to promote a high concentration of regenerators in the same specific nodes, whereas DLD tends to promote a slightly more homogeneous distribution of regenerators among the nodes.

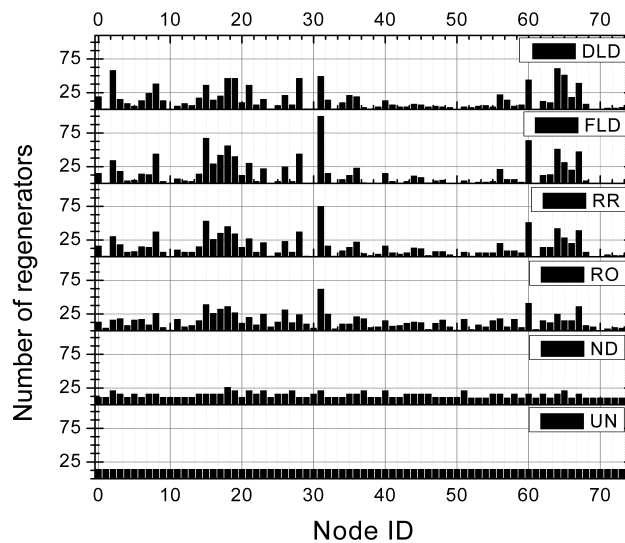


**Figure 4.** Number of regenerators placed by each considered RP algorithm in each network node of CoreNet assuming the uniform traffic and total amount of 1050 regenerators placed in the network.

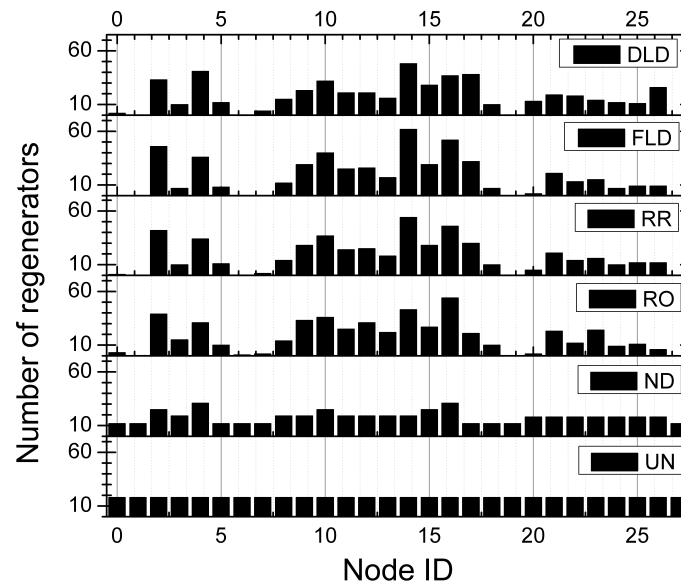


Figure 5. Number of regenerators placed by each considered RP algorithm in each network node of EuroNet assuming the uniform traffic and total amount of 504 regenerators placed in the network.

Figure 6 (Figure 7) shows the BP as a function of the total offered load in the CoreNet (EuroNet) topology under uniform (Figures 6a and 7a) and non-uniform. (Figures 6b and 7b) traffic profiles for the translucent solutions found by each algorithm with a total of 1050 (504) regenerators. Note that the DLD algorithm achieves the lowest BP values among all algorithms for both topologies under either UN or nUT traffic patterns and for the entire investigated load range. Moreover, in both topologies, the relative performance of the algorithms is almost unaltered in terms of BP as the obtained curves show almost no crossing points.

We can also analyze the EQU scenario against the DIF scenario in Figures 2, 3, 6 and 7 by comparing the lines against the symbols of the same color. Note that there are small differences in BP values by making this comparison for a given number of regenerators placed in the network. It means that the RPPs algorithms investigated are very robust against the investigated traffic changes. The premise of our algorithm is to solve the RPP problem to reduce the PB by using the information about the forecast traffic to the network. This is a valid premise as, frequently, there is an approximate information on the network traffic forecast. It makes sense, however, to consider that the actual network traffic be moderately different from the one forecast, but not completely different. With the provided results (i.e., comparison between the DIF and EQU scenarios), we show that, even for moderate differences between forecast and actual network traffic, the proposed RPP algorithms work satisfactorily.

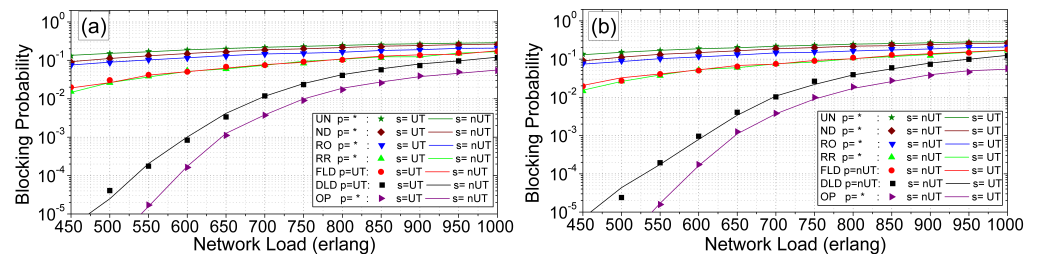
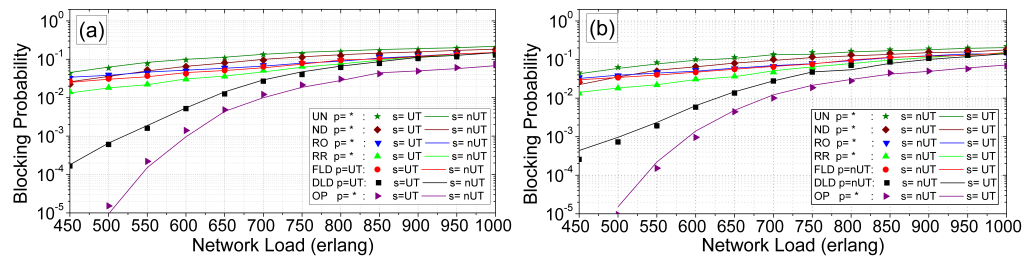


Figure 6. Blocking probability as a function of the total load in CoreNet topology using 1050 regenerators and traffic: (a) uniform and (b) non uniform.



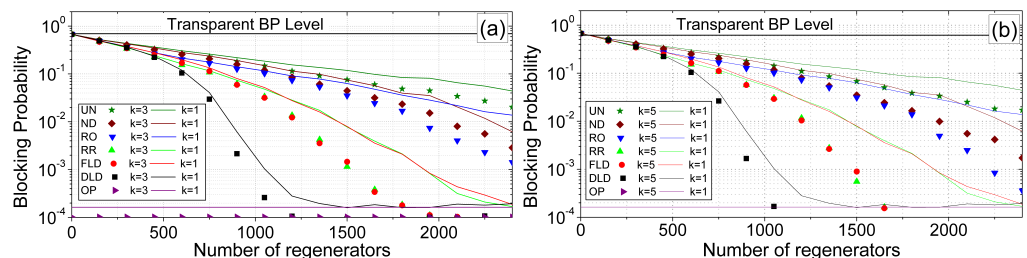


**Figure 7.** Blocking probability as a function of the total load in EuroNet topology using 504 regenerators and traffic: (a) uniform and (b) non uniform.

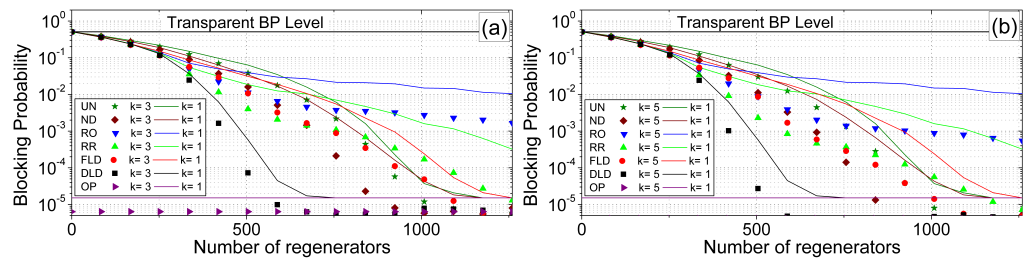
We also investigated the performance of the RPP algorithms when the network operates using the  $k$ -shortest path routing algorithm instead of the 1-shortest path (Dijkstra’s algorithm) assumed during the RPP procedure. In this case, the simulation is performed by trying, successively, each of the  $k$  shortest routes (in terms of distance) found by Yen’s  $k$ -shortest path routing algorithm. Figure 8 (Figure 9) shows BP as a function of the total number of regenerators installed in the CoreNet (EuroNet) topology. under UT and total offered load of 600 erl (500 erl).

Figure 8a (Figure 9a) stands for the comparison between the BPs verified using  $k = 3$  (shown as closed symbols) against the ones verified for  $k = 1$  (shown as lines), whereas Figure 8b (Figure 9b) stands for the comparison between the BPs verified using  $k = 5$  (closed symbols) against the ones verified for  $k = 1$  (lines). As expected, the greater the value of  $k$  considered, the lower the BP achieved by a given algorithm. In all investigated cases, the DLD algorithm remains the best cost-effective strategy to solve RPP regardless of the value of  $k$  selected. It means that, for a given number of regenerators, the DLD strategy always returns lower or equal BP when compared to the other strategies. Moreover, note that the relative performance of the algorithms, in terms of BP, remains almost unaltered by comparing their BPs results with  $k = 1$  against the BPs results using either  $k = 3$  or  $k = 5$ . It means that, for a given value of  $R$ , the algorithm that returns the lowest BP for  $k = 1$  also returns the lowest BP for both  $k = 3$  and  $k = 5$ . The same occurs with the algorithm that returns the second-lowest BP and so on. There are some exceptions, such as the comparison between ND and RO in CoreNet for a large number of 3R installed.

The performance of the RPP algorithms for different transparent reaches is also investigated. For this purpose, we have decided to show the results for the best (in terms of BP) 4 algorithms investigated so far: ND, RR, FLD, and DLD. We investigate the algorithms performance assuming 3 different transmissions reaches  $T_R$ :  $T_R = 1600$  km, 2000 km, and 2400 km. Notice that the  $T_R$  is an input parameter for the RPP algorithms RR, FLD, and DLD, as it is taken into account during the RPP procedure. Thus, different values of  $T_R$  require different execution of RR, FLD, and DLD.



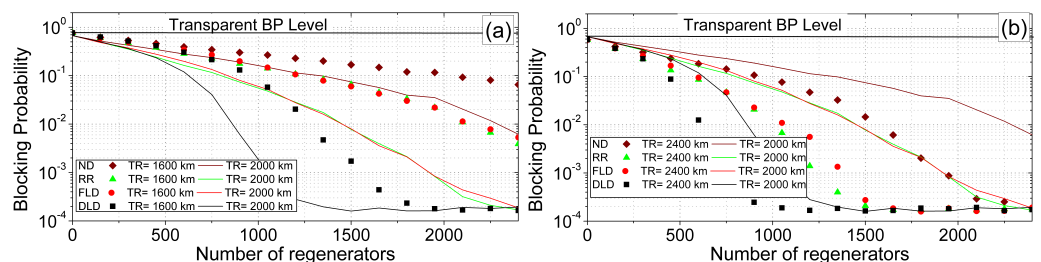
**Figure 8.** Blocking probability as a function of the total number of regenerators in CoreNet topology using  $k$ -shortest path routing algorithm for: (a)  $k = 3$ ; (b)  $k = 5$ , each compared against the  $k = 1$  case.



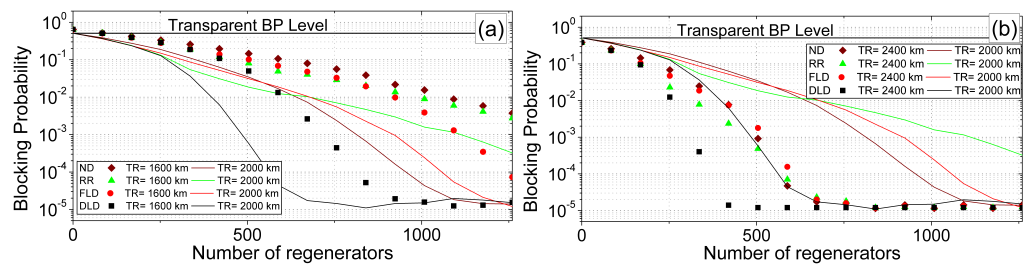
**Figure 9.** Blocking probability as a function of the total number of regenerators in EuroNet topology using k-shortest path routing algorithm for: (a)  $k = 3$ ; (b)  $k = 5$ , each compared against the  $k = 1$  case.

Figure 10 (Figure 11) shows BP as a function of the total number of regenerators installed in the CoreNet (EuroNet) topology under a uniform traffic and total offered load of 600 erl (500 erl). Figure 10a (Figure 11a) stands for the comparison between the BP verified assuming  $T_R = 1600$  km (shown as closed symbols) against the one verified for  $T_R = 2000$  km (shown as lines), whereas Figure 10b (Figure 11b) stands for the comparison between the BP verified assuming  $T_R = 2400$  km (closed symbols) against the one verified for  $T_R = 2000$  km (lines).

As expected, the greater the value of  $T_R$  considered, the lower the BP achieved by a given algorithm. In all investigated cases, the DLD algorithm remains the best cost-effective strategy to solve RPP regardless of the value of  $T_R$  selected. It means that, for a given number of regenerators, the DLD strategy always returns lower or equal BP when compared against the other strategies assuming the same  $T_R$ . On the other hand, the relative performance of the algorithms, ND, RR, and FLD, in terms of BP, shows significant dependence on the assumed  $T_R$ , mainly for a moderate/high number of regenerators installed in the network. In CoreNet, FLD and RR return almost the same values of BP in the entire considered range for  $R$  assuming both  $T_R = 1600$  km and  $T_R = 2000$  km (Figure 10a), whereas RR returns a slightly lower BP than FLD for  $T_R = 2400$  km and moderate values of  $R$  (Figure 10b). The most significant inversions are verified for the EuroNet. Assuming  $T_R = 2000$  km, ND returns lower BPs than RR and FLD for moderate to low numbers of  $R$  (compare the lines in Figure 11a,b). However, for  $T_R = 1600$  km ND returns the highest value of BP when compared to the ones returned by both RR and FLD for moderate to high values of  $R$ . Moreover, whereas FLD returns significantly lower BPs than RR for both  $T_R = 1600$  km and  $T_R = 2000$  km, RR returns slightly lower BP than FLD for  $T_R = 2400$  km.



**Figure 10.** Blocking probability as a function of the total number of regenerators in the CoreNet topology assuming transparent reaches of: (a)  $T_R = 1600$  km; (b)  $T_R = 2400$  km, each compared against the reach of  $T_R = 2000$  km.



**Figure 11.** Blocking probability as a function of the total number of regenerators in the EuroNet topology assuming transparent reaches of: (a)  $T_R = 1600$  km; (b)  $T_R = 2400$  km, each compared against the reach of  $T_R = 2000$  km.

Finally, we also investigated the number and the arrangement of the essential nodes in the analyzed topologies considering the transmission reaches of  $T_R = 1600$  km,  $T_R = 2000$  km, and  $T_R = 2400$  km, as shown in Table 1. In this table, we provide the number of essential nodes in each topology  $T_R$  scenario, as well as the node indexes of the essential nodes in the topologies. One can note that, as expected, the number of essential nodes reduces as the transmission reach increases. This occurs because the higher the transmission reach, the lower the number of required regeneration points along a given route.

**Table 1.** Total amount and node indexes of the essential nodes found for EuroNet and CoreNet topologies considering different transmission reaches of  $T_R = 1600$  km,  $T_R = 2000$  km, and  $T_R = 2400$  km.

Topology	$T_R$ (km)	Number of Essential Nodes	Index of the Essential Nodes
EuroNet	1600	19	2, 3, 4, 5, 6, 7, 9, 10, 11, 12, 14, 16, 17, 19, 20, 21, 23, 24, 26
EuroNet	2000	13	2, 4, 8, 10, 11, 14, 15, 16, 17, 20, 21, 22, 26
EuroNet	2400	4	9, 13, 16, 22
CoreNet	1600	42	0, 2, 3, 6, 7, 8, 11, 12, 13, 14, 15, 16, 17, 18, 19, 21, 22, 23, 25, 26, 27, 31, 32, 35, 36, 39, 41, 45, 46, 47, 52, 54, 56, 57, 60, 62, 63, 64, 65, 66, 67, 68
CoreNet	2000	28	0, 2, 3, 7, 8, 9, 12, 14, 15, 18, 19, 21, 23, 26, 28, 31, 35, 46, 56, 57, 59, 60, 62, 64, 65, 66, 67, 68
CoreNet	2400	17	0, 2, 3, 7, 9, 14, 18, 19, 21, 26, 28, 31, 32, 52, 56, 60, 65

### 7. Conclusions

In this paper, we propose two heuristic strategies to solve the regenerator placement problem (RPP) in translucent networks under dynamic traffic. The heuristics are based on both traffic forecasts and estimates of blocking probabilities in the network. The proposed heuristics are compared to other regenerator placement algorithms from the literature in two different typologies. We demonstrate the effectiveness of the new proposal under several different situations, such as uniform and non-uniform traffic, fixed and fixed alternative routing algorithms, different values of maximum transmission reach, as well as considering differences between forecast and actual network traffic.

From the obtained results, we conclude that the proposed DLD algorithm finds translucent networks with significant lower BP values than the other investigated algorithms in the paper for the same number of installed regenerators; regardless of the topology, traffic pattern, or intensity considered, transmission reach assumed and whether the fixed or fixed alternate routing is used during the network operation. The superior performance of the DLD algorithm over FLD can be explained by the fact that the DLD uses a more precise node load estimate.

On the other hand, the relative performance of the proposed FLD heuristic and the previously proposed RR, RO, ND, and UN heuristics are very dependent on the considered

scenario as the algorithm that achieves the lowest blocking probability values among them is strongly dependent on the topology, maximum transmission reach, number of regenerators deployed, and routing algorithm.

We also believe that the proposed algorithms/methodology can be extended for multi-rate/flex-grid networks by considering, for each rate, it is respective offered load and transmission reach as proposed in Appendix A.

**Author Contributions:** Conceptualization, A.L.S.d.F. and D.A.R.C.; Investigation, A.L.S.d.F. and D.A.R.C.; Methodology, A.L.S.d.F. and D.A.R.C.; Software, A.L.S.d.F. and D.A.R.C.; Validation, A.L.S.d.F., R.C.A.J. and D.A.R.C.; Writing—original draft, A.L.S.d.F., R.C.A.J. and D.A.R.C.; Writing—review & editing, A.L.S.d.F., R.C.A.J. and D.A.R.C. All authors have read and agreed to the published version of the manuscript.

**Funding:** This research was partially funded by Government Brazilian researching agencies National Council for Scientific and Technological Development (CNPq) and Fundação de Amparo à Ciência e Tecnologia de Pernambuco (Facepe).

**Acknowledgments:** The authors acknowledge the National Council for Scientific and Technological Development—CNPq, Facepe, University of Pernambuco, and Federal University of Pernambuco.

**Conflicts of Interest:** The authors declare no conflict of interest.

### Appendix A. Model Extension for Multi-Rate (Elastic) Networks

The formulation is shown in Sections 3 and 4 stands for networks under single bit-rate demands. We can also extend the formulation for a scenario with heterogeneous bit-rate demands. This is the case with elastic optical networks (EON) [11,34,35]. The extension starts by including an extra  $b$  sub-index to represent each possible transmission rate in the following symbols:  $\omega_{ijb}, \gamma_{ijb}, D_{ijb}, C_{ijb}, K_{ijb}, \Gamma_{nb}$ . The set  $U$  of allowable  $B$  bit rates is  $U = \{u_1, u_2, \dots, u_b, \dots, u_B\}$ . For instance,  $\omega_{ijb}$  represents the offered load of requests between the nodes  $i$  and  $j$  that requires a  $u_b$  transmission rate. To simplify the notation, we assume that the  $b$ -indexed transmission bit rate requires  $b$  regenerators to perform its regeneration. This is a valid consideration assuming the virtualized shared pool of elastic regenerators strategy proposed by Jinno et al. [34]. The elastic regenerators consist of an array of fixed-rate spectrum-selective subchannel regenerators (SSRs) that act as a pool of virtualized regeneration resources [34]. Each SSR operates under a fixed transmission bit rate.

Then, we use the theory of erlang loss systems under a multi-slot traffic [31] to evaluate the counterpart of the erlang-b formula under this multi-rate traffic scenario that occurs in EONs. Let us assume a node with  $s$  virtualized regenerators. A state  $e = (I_1, I_2, \dots, I_B)$  represents the number of active  $u_b$ -rate connections using SSRs in such a node, where  $I_b$  is the number of active  $u_b$ -rate connections, each of which, as explained before, using  $b$  regeneration resources. All possible states when  $s$  SSRs are installed in a node form the set  $\mathcal{E}_s$ , which includes any occurrence of values for  $(I_1, I_2, \dots, I_B)$  so that  $\sum_{b=1}^B b \cdot I_b \leq s$ . Let  $\mathcal{E}_s(b)$  be the set of states that cannot admit a  $u_b$ -rate demand, i.e.,  $\mathcal{E}_s(b) = \left\{ \forall e \mid \sum_{x=1}^B x \cdot I_x > s - b \right\}$ , as the summation accounts for the number of SSRs in use in the analyzed node and  $s - b$  accounts for the maximum number of SSRs in use in the node that still admits a regeneration of a  $u_b$ -rate demand in such node. In such scenario, we can replace (3) and (4) by

$$\Gamma_{nb} = \sum_{i=1}^N \sum_{j=1}^N E_{ijb}(n), \tag{A1}$$

in which  $E_{ijb}$  is a place holder for either  $G_{ijb}(n) = \gamma_{ijb}$  if  $\exists m / n \in c_{ijb}^{(m)}$  and 0 otherwise or for  $F_{ijb}$ :

$$F_{ijb}(n) = \begin{cases} \frac{\gamma_{ijb}}{M'_{ij}} \sum_{m=1}^{M'_{ij}} P_{ijm}(n), & \text{if } n \in \pi_{ij} \\ 0, & \text{otherwise,} \end{cases} \quad (\text{A2})$$

with  $P_{ijm}(n) = 1$  if  $n \in d_{ijb}^{(m)}$  and 0 otherwise.

In a node  $n$  with  $s$  SSRs, the probability of a state  $e \in \mathcal{E}_s$  is given by [31]

$$p_n(e, s) = Q_s \prod_{b=1}^B \frac{\Gamma_{nb}^{I_b}}{I_b!}, \quad (\text{A3})$$

in which  $\Gamma_{nb}$  is the total offered load estimate from  $u_b$ -rate demands on node  $n$  and  $Q_s$  is the normalization coefficient given by [31]

$$Q_s = \frac{1}{\sum_{e \in \mathcal{E}_s} p_n(e, s)}. \quad (\text{A4})$$

Then, the blocking probability of  $u_b$ -rate demands in node  $n$  may be evaluated by

$$BP_n(s, b) = \sum_{e \in \mathcal{E}_s(b)} p_n(e, s), \quad (\text{A5})$$

and (6) can be replaced by

$$BP_N(n, s) = \frac{\sum_{i=1}^N \sum_{j=1}^N \sum_{b=1}^B PB_n(s, b) \cdot E_{ijb}(n)}{\sum_{i=1}^N \sum_{j=1}^N \sum_{b=1}^B \omega_{ijb}}. \quad (\text{A6})$$

For a node  $n$  with a total of  $r(n)$  installed regenerators, it is possible to replace (8) in a multi-rate scenario using

$$\Delta BP_N(n, r(n)) = BP_N(n, r(n)) - BP_N(n, r(n) + 1). \quad (\text{A7})$$

## References

1. Yang, X.; Ramamurthy, B. Sparse Regeneration in Translucent Wavelength-Routed Optical Networks: Architecture, Network Design and Wavelength Routing. *Photonic Netw. Commun.* **2005**, *10*, 39–53. [CrossRef]
2. Pedro, J. Predeployment of regenerators for fast service provisioning in DWDM transport networks [Invited]. *J. Opt. Commun. Netw.* **2015**, *7*, A190–A199. [CrossRef]
3. Nath, I.; Chatterjee, M.; Bhattacharya, U. A survey on regenerator Placement Problem in translucent optical network. In Proceedings of the 2014 International Conference on Circuits, Systems, Communication and Information Technology Applications (CSCITA), Mumbai, India, 4–5 April 2014; pp. 408–413. [CrossRef]
4. Chaves, D.A.R.; Carvalho, R.V.B.; Pereira, H.A.; Bastos-Filho, C.J.A.; Martins-Filho, J.F. Novel strategies for sparse regenerator placement in translucent optical networks. *Photonic Netw. Commun.* **2012**, *24*, 237–251. [CrossRef]
5. da Silva, E.; Almeida, R.C., Jr.; Pereira, H.; Chaves, D. Assessment of novel regenerator assignment strategies in dynamic translucent elastic optical networks. *Photonic Netw. Commun.* **2020**, *39*, 54–69. [CrossRef]
6. Nath, I.; Bhattacharya, U.; Chatterjee, M. An Efficient Heuristic to Minimize Number of Regenerations in Translucent Optical Network under Dynamic Scenario. In Proceedings of the 20th International Conference on Distributed Computing and Networking, Bangalore, India, 4–7 January 2019; pp. 451–454. [CrossRef]
7. Chaves, D.A.R.; da Silva, E.F.; Bastos-Filho, C.J.A.; Pereira, H.A.; Almeida, R.C. Heuristic algorithms for regenerator assignment in dynamic translucent elastic optical networks. In Proceedings of the 2015 17th International Conference on Transparent Optical Networks (ICTON), Budapest, Hungary, 5–9 July 2015; pp. 1–4. [CrossRef]
8. De Groote, M.; Manousakis, K.; Kokkinos, P.; Colle, D.; Pickavet, M.; Christodoulouopoulos, K.; Varvarigos, E.; Demeester, P. Cost comparison of different translucent optical network architectures. In Proceedings of the 2010 9th Conference of Telecommunication, Media and Internet, Ghent, Belgium, 7–9 June 2010; pp. 1–8. [CrossRef]
9. Rahman, Q.; Bandyopadhyay, S.; Aneja, Y. Optimal regenerator placement in translucent optical networks. *Opt. Switch. Netw.* **2015**, *15*, 134–147. [CrossRef]
10. Leitner, M.; Ljubić, I.; Riedler, M.; Ruthmair, M. Exact Approaches for Network Design Problems with Relays. *INFORMS J. Comput.* **2019**, *31*, 171–192. [CrossRef]



11. Cavalcante, M.A.; Pereira, H.A.; Chaves, D.A.R.; Almeida, R.C. Evolutionary Multiobjective Strategy for Regenerator Placement in Elastic Optical Networks. *IEEE Trans. Commun.* **2018**, *66*, 3583–3596. [[CrossRef](#)]
12. Aibin, M.; Walkowiak, K. Regenerator placement algorithms for cloud-ready Elastic Optical Networks. In Proceedings of the 2015 17th International Conference on Transparent Optical Networks (ICTON), Budapest, Hungary, 5–9 July 2015; pp. 1–4. [[CrossRef](#)]
13. Chaves, D.A.R.; Ayres, C.F.C.L.C.; Carvalho, R.V.B.; Pereira, H.A.; Bastos-Filho, C.J.A.; Martins-Filho, J.F. Multiobjective sparse regeneration placement algorithm in optical networks considering network performance and CAPEX. In Proceedings of the 2010 12th International Conference on Transparent Optical Networks, Munich, Germany, 27 June–1 July 2010; pp. 1–4. [[CrossRef](#)]
14. Rizzelli, G.; Musumeci, F.; Tornatore, M.; Maier, G.; Pattavina, A. Wavelength-aware translucent network design. In Proceedings of the 2011 Optical Fiber Communication Conference and Exposition and the National Fiber Optic Engineers Conference, Los Angeles, CA, USA, 6–10 March 2011; pp. 1–3.
15. Agarwal, M.; Chatterjee, M.; Chandran, S. Offline routing and wavelength assignment for identification of regeneration sites in translucent WDM optical networks. In Proceedings of the 2017 International Conference on Advances in Computing, Communications and Informatics (ICACCI), Udipi, India, 13–16 September 2017; pp. 623–628. [[CrossRef](#)]
16. Li, X.; Aneja, Y. Regenerator location problem: Polyhedral study and effective branch-and-cut algorithms. *Eur. J. Oper. Res.* **2017**, *257*, 25–40. [[CrossRef](#)]
17. Mertzios, G.; Shalom, M.; Wong, P.; Zaks, S. Online Regenerator Placement. *Theory Comput. Syst.* **2017**, *61*, 739–754. [[CrossRef](#)]
18. Yan, L.; Xu, Y.; Brandt-Pearce, M.; Dharmaweera, N.; Agrell, E. Robust regenerator allocation in nonlinear flexible-grid optical networks with time-varying data rates. *IEEE/OSA J. Opt. Commun. Netw.* **2018**, *10*, 823–831. [[CrossRef](#)]
19. Li, X.; Aneja, Y. A new branch-and-cut approach for the generalized regenerator location problem. *Ann. Oper. Res.* **2020**, *295*, 229–255. [[CrossRef](#)]
20. Li, X.; Aneja, Y. A Branch-And-Benders-Cut approach for the fault tolerant regenerator location problem. *Comput. Oper. Res.* **2020**, *115*, 104847. [[CrossRef](#)]
21. Zhao, J.; Subramaniam, S.; Brandt-Pearce, M. Efficient and accurate analytical performance models for translucent optical networks. *J. Opt. Commun. Netw.* **2014**, *6*, 1128–1142. [[CrossRef](#)]
22. Chaves, D.A.R.; Cavalcante, M.A.; Pereira, H.A.; Almeida, R.C. A case study of regenerator placement and regenerator assignment in dynamic translucent elastic optical networks. In Proceedings of the 2016 18th International Conference on Transparent Optical Networks (ICTON), Trento, Italy, 10–14 July 2016; pp. 1–4. [[CrossRef](#)]
23. Walkowiak, K.; Klinkowski, M. Energy Efficiency of Dynamic Routing in Elastic Optical Networks with Back-to-Back Regeneration. In Proceedings of the 2018 International Conference on Computing, Networking and Communications (ICNC), Maui, HI, USA, 5–8 March 2018; pp. 399–403. [[CrossRef](#)]
24. Yang, H.; Zhao, X.; Yao, Q.; Yu, A.; Zhang, J.; Ji, Y. Accurate Fault Location using Deep Neural Evolution Network in Cloud Data Center Interconnection. *IEEE Trans. Cloud Comput.* **2020**. [[CrossRef](#)]
25. Leland, W.E.; Taqqu, M.S.; Willinger, W.; Wilson, D.V. On the self-similar nature of Ethernet traffic (extended version). *IEEE/ACM Trans. Netw.* **1994**, *2*, 1–15. [[CrossRef](#)]
26. Karagiannis, T.; Molle, M.; Faloutsos, M.; Broido, A. A nonstationary Poisson view of Internet traffic. In Proceedings of the IEEE INFOCOM 2004, Hong Kong, China, 7–11 March 2004; Volume 3, pp. 1558–1569. [[CrossRef](#)]
27. Terdik, G.; Gyires, T. Does the Internet Still Demonstrate Fractal Nature? In Proceedings of the 2009 Eighth International Conference on Networks, Guadeloupe, France, 1–6 March 2009; pp. 30–34. [[CrossRef](#)]
28. Terdik, G.; Gyires, T. LEvy Flights and Fractal Modeling of Internet Traffic. *IEEE/ACM Trans. Netw.* **2009**, *17*, 120–129. [[CrossRef](#)]
29. Walkowiak, K.; Klinkowski, M.; Włodarczyk, A.; Kasprzak, A. Predeployment of transponders for dynamic lightpath provisioning in translucent spectrally-spatially flexible optical networks. *Appl. Sci.* **2020**, *10*, 2802. [[CrossRef](#)]
30. Cheng, S.; Xiao, D.; Huang, A.; Aibin, M. Machine learning for regenerator placement based on the features of the optical network. In Proceedings of the 2019 21st International Conference on Transparent Optical Networks (ICTON), Angers, France, 9–13 July 2019. [[CrossRef](#)]
31. Anurag Kumar, D.M.; Kuri, J. *Communication Networking: An Analytical Approach*, 1st ed.; Morgan Kaufmann: Burlington, MA, USA, 2004.
32. DARPA. Core Optical Networks (CORONET) Continental United States (CONUS) Topology. Available online: [http://monarchna.com/CORONET\\_CONUS\\_Topology.xls](http://monarchna.com/CORONET_CONUS_Topology.xls) (accessed on 1 January 2018).
33. Cavalcante, M.; Pereira, H.; Chaves, D.; Almeida, R. Optimizing the cost function of power series routing algorithm for transparent elastic optical networks. *Opt. Switch. Netw.* **2018**, *29*, 57–64. [[CrossRef](#)]
34. Jinno, M.; Takara, H.; Yonenaga, K.; Hirano, A. Virtualization in optical networks from network level to hardware level. *J. Opt. Commun. Netw.* **2013**, *5*, A46–A56. [[CrossRef](#)]
35. Yang, H.; Yao, Q.; Bao, B.; Yu, A.; Zhang, J.; Vasilakos, A.V. Multi-Associated Parameters Aggregation-Based Routing and Resources Allocation in Multi-Core Elastic Optical Networks. *IEEE/ACM Trans. Netw.* **2022**, 1–13. [[CrossRef](#)]